IVYSPRING INTERNATIONAL PUBLISHER

International Journal of Biological Sciences

2019; 15(6): 1161-1176. doi: 10.7150/ijbs.32004

Research Paper

Hypoxia preconditioned renal tubular epithelial cell-derived extracellular vesicles alleviate renal ischaemia-reperfusion injury mediated by the HIF-1α/Rab22 pathway and potentially affected by microRNAs

Lei Zhang[1,2*], Han Liu[3*], Kai Xu[2*], Zhixin Ling[4*], Yeqing Huang[5], Qiang Hu[1,2], Kai Lu[1,2], Chunhui Liu[1], Yiduo Wang[1,2], Ning Liu[1], Xiaowen Zhang[1], Bin Xu[1,2], Jianping Wu[1], Shuqiu Chen[1], Guangyuan Zhang[1,2]✉, Ming Chen[1,2]✉

1. Department of Urology, Zhongda Hospital, Southeast University, Nanjing, Jiangsu 210009, P.R. China;
2. Institute of Urology, Surgical Research Center, School of Medicine, Southeast University, Nanjing, Jiangsu 210009, P.R. China;
3. Department of Respiratory Medicine, The First Hospital of Jilin University, Changchun, Jilin 130000, P.R. China;
4. Department of Urology, The First Affiliated Hospital of Soochow University, Suzhou, Jiangsu 215006, P.R. China.
5. Department of Urology, The Affiliated Hospital of Nantong University, Nantong, Jiangsu 226001, P.R. China.

* Equal contributors

✉ Corresponding author: Ming Chen or Guangyuan Zhang, Department of Urology, Zhongda Hospital, Southeast University, 87 Dingjiaqiao, Gulou, Nanjing, Jiangsu 210009, P.R. China. E-mail: chenmingseu@126.com (M. Chen), zgy0879@qq.com (G. Zhang).

© Ivyspring International Publisher. This is an open access article distributed under the terms of the Creative Commons Attribution (CC BY-NC) license (https://creativecommons.org/licenses/by-nc/4.0/). See http://ivyspring.com/terms for full terms and conditions.

Received: 2018.12.04; Accepted: 2019.04.16; Published: 2019.05.07

Abstract

We previously found that hypoxia induced renal tubular epithelial cells (RTECs) release functional extracellular vesicles (EVs), which mediate the protection of remote ischaemic preconditioning (RIPC) for kidney ischaemia-reperfusion (I/R) injury. We intend to investigate whether the EVs were regulated by hypoxia-inducible factor 1α (HIF-1α) and Rab22 during RIPC. We also attempted to determine the potentially protective cargo of the EVs and reveal their underlying mechanism. Hypoxia preconditioning (HPC) of human kidney 2 (HK2) cells was conducted at 1% oxygen (O_2) for different amounts of time to simulate IPC in vitro. EVs were isolated and then quantified. HIF-1α- and Rab22-inhibited HK2 cells were used to investigate the role of the HIF-1α/Rab22 pathway in HPC-induced EV production. Both normoxic and HPC EVs were treated in vivo to assess the protective effect of I/R injury. Moreover, microRNA (miRNA) sequencing analysis and bioinformatics analysis was performed. We revealed that the optimal conditions for simulating IPC in vitro was no more than 12 h under the 1% O_2 culture circumstance. HPC enhanced the production of EVs, and the production of EVs was regulated by the HIF-1α/Rab22 pathway during HPC. Moreover, HPC EVs were found to be more effective at attenuating mice renal I/R injury. Furthermore, 16 miRNAs were upregulated in HPC EVs. Functional and pathway analysis indicated that the miRNAs may participate in multiple processes and pathways by binding their targets to influence the biochemical results during RIPC. We demonstrated that HIF-1α/Rab22 pathway mediated RTEC-derived EVs during RIPC. The HPC EVs protected renal I/R injury potentially through differentially expressed miRNAs. Further study is needed to verify the effective EV-miRNAs and their underlying mechanism.

Key words: extracellular vesicles, ischaemic preconditioning, ischaemia-reperfusion injury, hypoxia, microRNA

Introduction

Renal ischaemia-reperfusion (I/R) injury, the major cause of acute kidney injury (AKI), is a severe complication after major surgery and kidney transplantation. In addition, it is associated with increased morbidity and mortality[1,2]. Therefore, it is imperative to develop potent interventions to prevent

ischaemia-induced acute kidney injury.

Ischaemic preconditioning (IPC), which was first described in the heart by Murry et al. [3], consists of short sublethal cycles of ischaemia-reperfusion prior to the prolonged ischaemic insult. Subsequently, the phenomenon in which IPC of one organ was observed to protect remote organs, was defined as remote ischaemic preconditioning (RIPC) [4]. Currently, RIPC represents a more clinically practical strategy for limiting organ injury that has been successfully applied to the protection of cardiac, renal, and other organs against I/R injury [5,6]. However, its mechanism is still largely unknown and has attracted much attention in recent years.

A number of different mechanisms have been suggested, including roles for humoral mediators and neurally mediated mechanisms. As novel circulating mediators, extracellular vesicles (EVs) have recently been proposed to mediate the cardioprotection of RIPC [7,8]. EVs are membrane-bound vesicles secreted from almost all cell types, which can modulate intercellular communication by transfer of their bioactive cargos [9]. According to different sizes and intracellular origins, EVs can be characterised into different categories, but two major subsets capture most of the interest: namely exosomes (30–150 nm diameter, which are derived from multivesicular bodies (MVBs)) and microvesicles (MVs) (100–1,000 nm diameter, which are shed from the plasma membrane) [10].

In our previous work [11], we established a new animal model of RIPC firstly, which was IPC for right kidney protecting against I/R injury of left kidney. We found that hypoxia induced renal tubular epithelial cells (RTECs) to release functional EVs, which mediated the alleviation of kidney I/R injury.

Here, to push our investigations further, we sought to answer two questions. Firstly, how does the hypoxia during RIPC regulate the secretion of EVs? Hypoxia is a central component of ischaemia, and the hypoxia-inducible factor 1α (HIF-1α) transcription factor plays a crucial role in coordinating the transcriptional response to hypoxia [12]. HIF-1α-mediated organ protection in RIPC has been demonstrated both pre-clinically and clinically [13,14]. Recent studies have indicated that hypoxia enhanced secretion of EVs in cancer cells in an HIF-1α-dependent manner [15,16].

Moreover, Rab22 (also known as Rab22a), one of the small GTPases, has been found to be a downstream target of HIF-1α, and facilitates the shedding of breast cancer cells by MVs [16]. Actually, small GTPases of the Rab subfamily are involved in regulation of intracellular membrane trafficking events. To date, approximately 70 distinct Rab proteins have been identified in human systems with different Rab proteins being specific for distinct pathways that regulate the transport, docking and fusion of vesicles [17]. With reference to vesicular secretion, Rab11, Rab27 and Rab35 have been found to be involved in exosomal release via exocytosis in different cell lines in the former studies [18], while Rab22 has been found to localise to endosomal compartments and to the plasma membrane and play a major role in endosomal function endocytic and phagocytic pathways [18,19]. Here, enlighten by Wang's study [16], we assume that the expression of Rab22 in RTECs is positively correlated with HIF-1α and the productions of RTEC-derived EVs are mediated by HIF-1α/Rab22 pathway during RIPC.

EVs are believed to exert their functions by transfer their cargos to receptor cells. We supposed that the RIPC-induced EVs act as a protective role by changing their contents under hypoxia. Thus, the second question is whether the cargo changes of the RIPC induced EVs. The cargos of EVs are complex, including a great diversity of proteins, lipids and nucleic acids that can act as messengers for cell contacting [20,21]. RNAs are proved to be the major bioactive cargos in EVs, along with some kinds of non-coding RNAs, including microRNAs (miRNAs), long non-coding RNAs (lncRNAs), and circular RNAs (circRNAs) [22]. Among them, miRNAs are the most widely studied in the past years. We focused on miRNAs because both previous results and our study show the particular enrichment of miRNAs in EVs [11,23]. Additionally, the roles of miRNAs in I/R injury have been gradually revealed recent years. Some of them were reported to alleviate I/R injury, such as miR-132, miR-21 and miR-489 [24-26], while some were proven to aggravate the injury, such as miR-24, miR-218 and miR-128-3p [27-29]. Hence, we attempted to determine whether the changes of the miRNA profile in RIPC induced EVs, while the potentially functional miRNAs require further study.

Therefore, in the present study, we aimed to investigate whether the RTEC-derived EVs are regulated by the HIF-1α/Rab22 pathway during the RIPC process. In addition, miRNA sequencing analysis and bioinformatics analysis were performed to find potentially protective miRNAs and their mechanism.

Materials and methods

Animal experiments

All animal experiments were performed on male C57BL/6 mice, weighing 20-25g (10-12 weeks of age), obtained from the Comparative Medicine Centre of Yangzhou University (Yangzhou, China). Mice were

housed at a constant temperature, with a 12:12 h light-dark cycle and free access to water and rodent food. All protocols were approved by the Committee on the Ethics of Animal Experiments of Southeast University (Nanjing, China). All surgeries were performed under intraperitoneal sodium pentobarbital anaesthesia, and all efforts were made to minimise suffering.

RIPC was performed on the right kidneys after performing a back midline incision. For induction of RIPC, the right renal artery underwent 3 cycles of 5 min of ischaemia and 5 min of reperfusion using non-traumatic microvascular clamps. Mice were killed 10 min, 30 min and 24 h after reperfusion; and their bilateral kidneys and blood were collected for examination. For induction of IR, bilateral kidney was subjected to ischaemia for 35 min. For the treatment of renal I/R injury, PKH26-labelled EVs (50 μg suspended in 100 μl PBS) were injected intravenously 24 h before the operation of IR. Mice were killed 24 h after reperfusion, and their kidneys and blood were collected for examination.

Cell culture

Human RTECs (HK-2 cells) were obtained from a commercial source (Shanghai Institutes for Biological Sciences, Shanghai, China) cultured in Dulbecco's Modified Eagle Medium/Nutrient Mixture F-12 (DMEM/F12) medium (Thermo Fisher, Grand Island, NY, USA) supplemented with 10% foetal bovine serum (FBS) (ExCell Bio, Shanghai, China), 100 μg/ml streptomycin and 100 U/ml penicillin, (Gibco, Thermo Fisher) within a humidified atmosphere containing 5% CO_2 at 37℃. For EV isolation, cells were cultured in conditioned media supplemented with exosome-depleted FBS (System Biosciences, Palo Alto, CA, USA). Cell counts and quantification were performed using a hemocytometer, and viability was determined by 0.1% (w/v) Trypan blue (Sigma-Aldrich, Merck KGaA, Darmstadt, Germany) exclusion.

Hypoxic preconditioning

Hypoxic preconditioning (HPC), simulating IPC *in vitro*, was conducted within a hypoxic chamber at 1% O_2 and 37℃ in a 5% CO_2 humidified environment with the balance provided by nitrogen. The oxygen tension in the chamber was monitored and maintained by a computerised sensor probe. The time of HPC time was according to the experimental design.

Cell transfection and reagents

Cell transfection was performed with Lipofectamine 2000 (Invitrogen; Thermo Fisher) according to the manufacturer's protocol. Briefly, cells were seeded in a 10-cm dish at 70% confluence one day prior to transfection. Nucleotides formed transfection complexes with Lipofectamine 2000, and were added to cells and incubated for 6-8 h prior to refreshing the medium. Small interfering RNAs (siRNAs) were synthesised by GenePharma Co., Ltd., (Shanghai, China) based on the following sequences: HIF-1α siRNA: sense 5' CCAACCUCAGUGUGGGU AUdTdT 3' and antisense 5' AUACCCACACUGA GGUUGGdTdT 3', and Rab22 siRNA: sense 5' GGAUACAGGUGUAGGUAAAdTdT 3' and antisense 5' UUUACCUACACCUGUAUCCdTdT 3'. FAM labeled siRNA was used to assess the efficiency of transfection. Cells which expressed green fluorescence stably were considered to successful transfection. The efficiency of transfection was more than 90% (Figure S1).

Cell terminal deoxynucleotidyl transferase dUTP nick end labelling (TUNEL) assay

To label nuclei of apoptotic cells, HK2 cells were plated on glass coverslips in a 35-mm dish under different treatment conditions, and then fixed in 4% paraformaldehyde post-treatment. An In Situ Cell Death Detection Kit (Roche, Mannheim, Germany) was used to perform the terminal TUNEL staining, according to the manufacturer's protocol. The number of TUNEL-positive nuclei was counted and divided by the number of 4',6-diamidino-2-phenylindole (DAPI)-stained nuclei to calculate the percentage of TUNEL-positive cells.

Cell immunofluorescence assay

Different treated HK2 cells, plated on glass coverslips in a 35-mm dish were fixed with 4% paraformaldehyde, permeabilised with 0.2% Triton X-100 and blocked with 10% bovine serum albumin (BSA). The cells were then incubated with primary antibodies: monoclonal mouse anti-human HIF-1α (ab1, Abcam, Cambridge, MA, USA) and monoclonal rabbit anti-human RAB22A antibodies (ab137093, Abcam); followed by incubation with secondary antibodies: Cy3-conjugated goat anti-mouse immunoglobulin G (IgG, GB21301, ServiceBio, Wuhan, China) and fluorescein isothiocyanate (FITC)-conjugated goat anti-rabbit IgG (GB22303, ServiceBio). DAPI, (G1012, ServiceBio) was used to stain nuclei. The samples were visualised using the Pannoramic 250 Flash series digital scanner and software (3DHistech, Budapest, Hungary).

Immunohistochemical (IHC) staining

The IHC kit (G1210, ServiceBio) was used for IHC staining. Kidney tissues were fixed in 4% paraformaldehyde (pH 7.4) and embedded in

paraffin, and then cut into 4-μm thicknesses. The sections were incubated with primary antibodies: monoclonal mouse anti-human HIF-1α (1:100, ab1, Abcam) and polyclonal rabbit anti-human RAB22A (1:50, 12125-1-AP, Proteintech, Rosemont, IL, USA) at 4 ℃ overnight. After washing with phosphate-buffered saline (PBS), the sections were then incubated with horseradish peroxidase (HRP)-conjugated IgG for 30 min, followed by 3,3'-diaminobenzidine (DAB). Finally, the sections were counterstained with haematoxylin. The staining intensity of HIF-1α and RAB22A was assessed by two independent pathologists.

Periodic acid–Schiff (PAS) staining

To detect renal injury, kidneys were fixed in 4% paraformaldehyde (pH 7.4), gradually dehydrated, embedded in paraffin, cut into 4-μm sections and subjected to PAS staining. Histopathological scoring was conducted in a blinded manner and given based on grading of tubular cell necrosis or swelling, tubular casts, brush border loss and interstitial infiltration by multi-nucleated cells in 10 randomly chosen, non-overlapping fields (200× magnification). According to the severity of changes on a semi-quantitative scale, scores were given as follows: 0 was no injury, 1 mild, 2 moderate, 3 severe and 4 very severe.

Plasma creatinine assay

Blood samples were obtained through cardiac puncture at the indicated times. Plasma creatinine was measured using the sarcosine oxidase method by a commercial creatinine assay kit (C011-2, NJJC-Bio, Nanjing, China).

Extracellular vesicle extraction

After culture in the presence or absence of hypoxia, conditioned medium was carefully collected and subjected to a series of centrifugation at 800 g for 10 min, 2,000 g for 20 min and 10,000 g for 30 min at constant 4℃. The resultant supernatant was finally subjected to ultracentrifugation in a SW41 swing rotor (Beckman Coulter, Fullerton, CA, U.S.) for 1 h at 4℃ to collect EVs in pellets. EV pellets were resuspended in 100 μl of particle-free PBS for subsequent assays immediately or stored at 4℃ short-term (1-7 days) or -20℃ long-term. Cell counts and viability were also determined at the time of harvest as described above to account for differences in cell growth and normalisation of the cell numbers.

Nanoparticle tracking analysis(NTA)

We completed NTA with ZetaView PMX 110 (Particle Metrix, Meerbusch, Germany) and corresponding software ZetaView 8.04.02 SP2. To analyse the size distribution and concentration of the EVs. Isolated EVs were appropriately diluted in particle-free PBS and resuspended before being injected into the sample cell chamber. Size distributions and particle concentrations were assessed at 11 positions. Polystyrene particles sized 110 nm were used to calibrate the ZetaView system. Temperature was maintained around 23℃ and 37℃. EV concentration analysis was normalised with the total number of cells from the corresponding dish.

Transmission electron microscopy (TEM)

TEM was conducted by the Electron Microscopy Core of Southeast University. Ten microlitres of EV pellet solution was loaded onto a formvar/carbon-coated 200-mesh copper electron microscopy grid, incubated at room temperature for 5 min and then subjected to negative staining with 3% aqueous phosphor-tungstic acid for 1 min. The grid was washed with particle-free PBS and allowed to semidry at room temperature before observation in transmission electron microscope (HITACHI H7650 TEM; Tokyo, Japan).

Flow cytometry (FCM) analysis

For detecting EVs with FCM, the EVs that were resuspended in PBS were stained by the EVs-specific antibodies: FITC-conjugated anti-CD63 (557288, BD, San Jose, CA, USA), FITC-conjugated anti-CD81 (557288, BD) for positive staining, or FITC-conjugated IgG1 (ab91356, Abcam) as a negative control. The fluorescence-labelled EVs were analysed with an Accuri C6 flow cytometer (BD).

Western blotting analysis

Cell lysate and EV proteins were extracted with ice-cold radioimmunoprecipitation assay (RIPA) buffer. Protein concentration was quantified with a BCA Protein Assay Kit (Keygen Biotech, Nanjing, China). Total EV proteins loading for Western blot were normalised with the total cell number of the corresponding dishes as described above. Protein was separated by 10% sodium dodecyl sulfate-polyacrylamide gel electrophoresis and transferred to a polyvinylidene difluoride membrane (MilliporeSigma, Burlington, MA, USA) The membrane was blocked with 5% BSA for 1 h at room temperature and then immunoblotted with primary antibodies at 4℃ overnight. The blot membrane was then washed three times and incubated with secondary antibodies at 37℃ for 1 h. The blot signal was revealed with enhanced chemiluminescence (ECL, Beyotime, Shanghai, China). Primary antibodies used were monoclonal rabbit anti-human

HIF-1α (1:500, ab51608, Abcam), monoclonal rabbit anti-human RAB22A (1:2000, ab137093, Abcam), polyclonal rabbit anti-human HSP70 (1:1000, 10995-1-AP, Proteintech), monoclonal mouse anti-human TSG101 (1:1000, MA1-23296, Thermo Fisher) and monoclonal mouse anti-human β-actin (1:3000, 7D2C10, Proteintech). Secondary antibodies used were HRP-labelled anti-rabbit IgG (1:3000, #7074, Cell Signalling Technology, Danvers, MA, USA) and HRP-labeled anti-mouse IgG (1:3000, #7076, Cell Signalling Technology).

Quantitative analyses of EVs

We quantified the production of EVs mainly by EV-specific protein quantification. To increase the accuracy of quantitative analysis, enzyme-linked immunosorbent assay (ELISA) and western blot, these two methods were both used. For ELISA analysis, we used an ExoTEST™ kit for detecting CD9-positive EVs (exosomes) which was purchased from HansaBioMed (Tallinn, Estonia). The assays were performed in accordance with the manufacturer's instructions. For western blot, we used the protein levels of HSP70 as the indicator of EV quantity. Western blotting analysis was conducted as described above.

MicroRNA library construction and sequencing

To analyse RNA contents in EVs, a Qiagen RNA isolation kit was used to extract total RNA and RNA was analysed using the Agilent 2100 bioanalyser (Agilent Tech, U.S.). MiRNA profiling of EVs from normoxic and IPC HK2 cell culture medium was performed by the Professional Ribo Biotech Corporation (Guangzhou, China). Briefly, total RNA samples were fractionated on a 15% Tris-borate-EDTA (TBE) polyacrylamide gel (Invitrogen, Thermo Fisher) and small RNAs ranging between 18 and 30 nucleotides (nt) were used for library preparation. Small RNAs were reverse transcribed and amplified by polymerase chain reaction (PCR). The PCR products were sequenced using the Illumina HiSeq 2500 platform. The filtering criteria for up or downregulated genes were fold change of ≥ 2 and $P < 0.05$.

Bioinformatics analysis

The putative target genes of miRNAs were determined through examination of the overlapped intersection from 3 databases (miRDB, TargetScan and miRWalk). Gene ontology (GO) and the Kyoto Encyclopaedia of Genes and Genomes (KEGG) were utilized to analyse the main function and significant pathways of the selected putative target genes. The filtering criterion of significance was defined as $P < 0.05$ for both GO and KEGG analyses. The potential regulatory networks between miRNAs and target genes were assembled and visualised using Cytoscape software. A directed edge (connection) from a miRNA to one of its targets exists if their relationship is functionally regulated. We then calculated the degree of the network that was defined as the number of neighbours (edges) of a node. The higher degree of connectivity that a given node has, the more biologically important role it plays in the regulatory network.

Statistical analysis

All dates are expressed as means ± SD. Statistical analysis was conducted using SPSS 16.0 statistical software. Comparisons between two groups were performed by Student's t-test. For multiple comparisons, analysis of variance (ANOVA) was used, followed by post-hoc analysis using the least significant difference (LSD). $P < 0.05$ was considered statistically significant. Each experiment was conducted independently at least three times.

Results

Optimal conditions for simulating IPC in vitro with HK2 cells were no more than 12 h under the 1% oxygen culture circumstance

We screened the optimal conditions for simulating IPC in vitro with HK2 cells mainly through biological changes, such as cell morphology, proliferation, apoptosis and the activation of HIF-1α. HK2 cells were divided to different groups, and HPC in 1% oxygen content environment from 0-72 h (Fig. 1a). We observed the gradual morphological changes of cells under the hypoxic environment after 24 h. Cells changed from a regular long spindle shape to irregular, disorganised shapes (Fig. 1b). Moreover, the number of cells significantly decreased as the hypoxic time increased, which reflected that prolonged hypoxic time influenced cell proliferation (Fig. 1c). There was no significant effect on cell apoptosis within 24 h, but significant apoptosis occurred in cells after 1% hypoxia more than 24 h (Fig. 1d and e). The expression level of HIF-1α was tested by western blot. With the prolongation of hypoxic time, the accumulation of HIF-1α in the cell reached a peak within 12 h. The increase of hypoxic time after 12 h did not increase the expression, while HIF-1α gradually degraded (Fig. 1f and g). In summary, through the above investigations, we believe that the optimal conditions for the simulation of IPC with HK2 cells should be no more than 12 h in a 1% oxygen content environment.

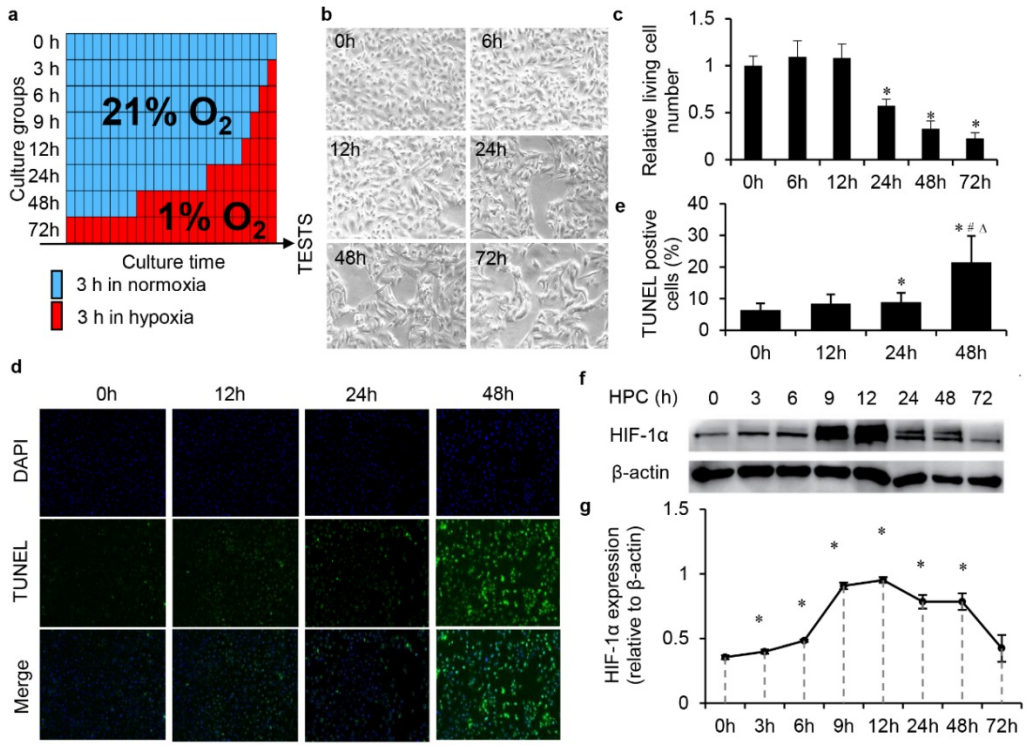

Figure 1. Optimal condition screening for simulating IPC in vitro with HK2 cells under the 1% oxygen culture circumstance. (a) Schema of the protocols of screening for optimal conditions of simulating IPC in vitro with HK2 cells. (b) Morphology and amount changes of cells under the hypoxic environment, magnification 200×. (c) The relative living cell numbers in each group, (* P<0.05 compare with 0 h). (d) Cell TUNEL assay and (e) the quantification (*, #, Δ, P<0.05 compare with 0 h, 12 h, 24 h, respectively). (f) HIF-1α was tested by western blot and (g) semi-quantification (* P<0.05 compare with 0 h).

The changes of EVs production and characterisation after HPC

EVs were isolated from the conditioned media of HK2 cells by serial low speed centrifugation followed by ultracentrifugation.

Firstly, we examined the impact of HPC on EVs secretion in HK2 cells. The cells were exposed to normoxia or IPC for 6, 12 and 24 h. ELISA analysis indicated that the yield of CD9-positive EVs increased with the time of HPC. This trend reached a significant difference, particularly at 12 h and 24 h, respectively, 2.13-fold and 2.34-fold higher than normoxia (Fig. 2a). This time dependence was expected because more EVs were secreted into culture medium as the hypoxic incubation time increased. Our western blot analysis also showed a time-dependent increase of EV protein HSP70 under IPC, and this increase did not achieve statistical significance until 12 h (Fig. 2b, c). Therefore, to conduct follow-up analysis, we divided the EVs into the normoxia and HPC groups, and the EVs obtained from conditioned medium under the HPC environment for 12 h were selected to represent the HPC group for the above reasons.

Furthermore, a serial of analysis was conducted to investigate the characterisation of normoxic and HPC EVs. Transmission electron microscopy revealed the both groups of EVs exhibited similar morphologies as round- ("cup") or oval-shaped ("dish") lipid bilayer vesicles (Fig. 2d). Samples examined by NTA showed that the size ranged from 30-500 nm in both groups. However, mean size was 149·43±4·87nm (normoxia) and 173·90±3·30 (IPC), respectively. Both groups exhibited a peak at 120 nm, while another distinct peak at 240 nm was observed in HPC sample (Fig. 2e). Such results seemed to indicate that increased EVs produced in the HPC environment mainly concentrated in the size of 240 nm, which mainly belonged to MVs rather than exosomes. We also characterised four protein markers of EVs by FCM analysis and western blot analysis. FCM analysis detected CD63 and CD81, two widely accepted markers of EVs, in the isolated samples. As shown in Fig. 2f, the proteins of CD63 and CD81were positively expressed in normoxic or HPC EVs. Western blot of EV fractions confirmed the presence of the EVs proteins HSP70 and TSG101 (Fig. 2g). As expected, the HPC EV sample showed higher content of HSP70 and TSG101 than that of normoxia after normalisation with equal cell numbers (Fig. 2h). Moreover, more total RNAs could be extracted form HPC EV samples than normoxic ones after cell number normalisation. Bioanalyser profile of EVs showed the presence of different subsets of RNAs and, in particular, enrichment for small RNAs (about 25 nt) (data not shown).

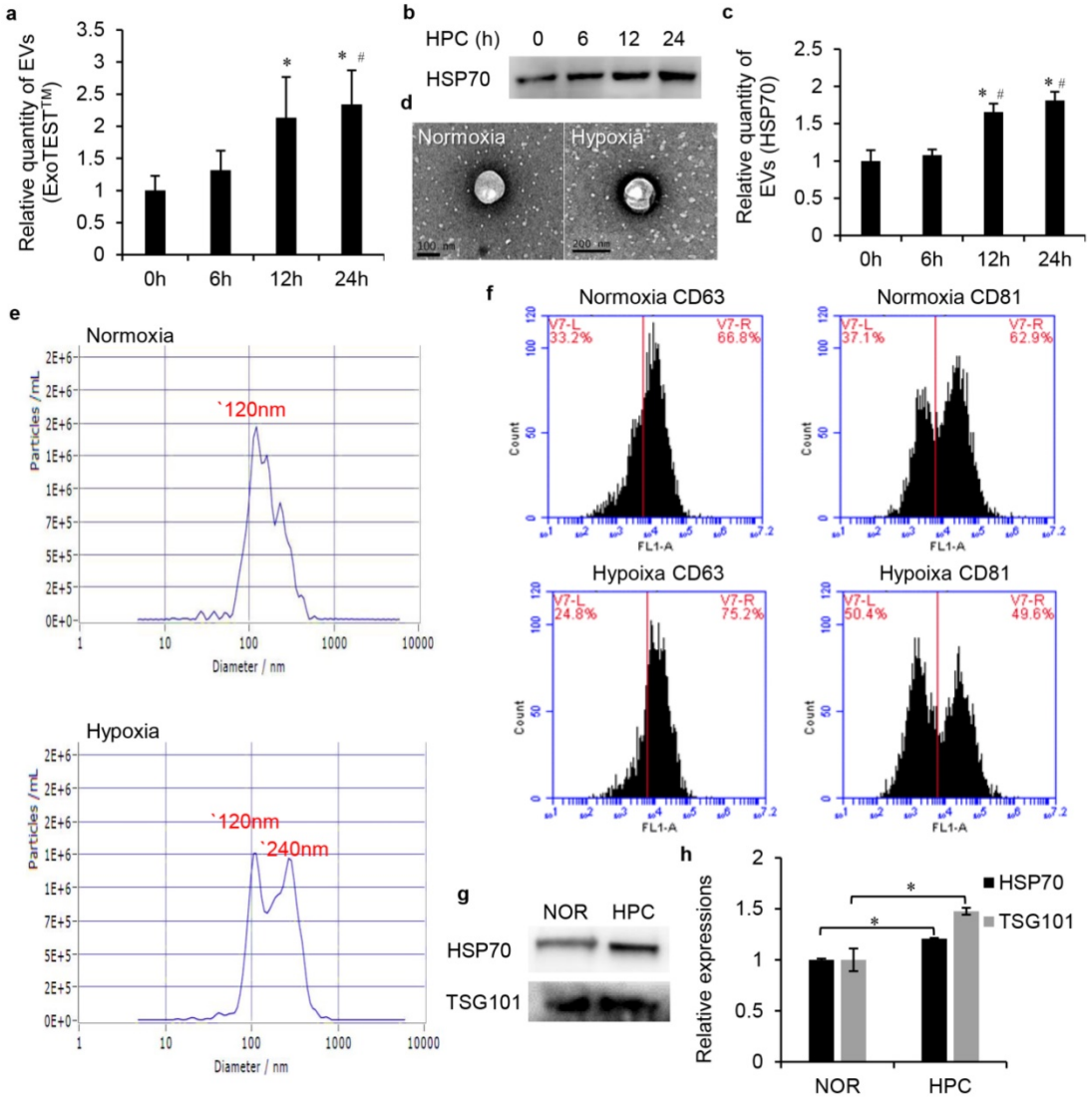

Figure 2. The changes of EV production and characterisation after HPC. (a) Relative quantity of EVs, ExoTESTTM method (*, #, P<0.05 compared with 0 h, 6 h, respectively). (b) EVs protein HSP70 western blot analysis and (c) semi-quantification (*, #, P<0.05 compared with 0 h, 6 h, respectively). (d) TEM assay. (e) NTA assay. (f) The proteins of CD63 and CD81were detected by FCM analysis. (g) Western blot of EV fractions confirmed the presence of the EV proteins HSP70 and TSG101 and (h) semi-quantification after normalisation with equal cell numbers (* P<0.05).

These results not only verify our EV isolation protocol but also indicate that HPC can enhance the EV production of HK2 cells and influence some characteristics of EVs.

The production of EVs was regulated by the HIF-1α/Rab22 pathway during IPC

IPC-enhanced Rab22 expression was HIF-1α-dependent in vivo and in vitro. IHC was conducted to detect HIF-1α and Rab22 protein expression in the IPC and sham mice kidneys. Results showed that HIF-1α was expressed strongly in IPC renal tubules with the expression of Rab22 enhanced accordingly. These 2 proteins showed a synchronic expression in vivo (Fig. 3a, b). Furthermore, HK2 cells were exposed to normoxia or HPC, harvested and tested at different time points. Both western blot analysis (Fig. 3c, d) and immunofluorescent assay (Fig. 3e, f) revealed that hypoxic exposure gradually affected the expression of HIF-1α and Rab22 in cells, and both of them peaked at the time point of HPC for 12 h but decreased at HPC for 24 h. These results were in agreement with the results in vivo. To further prove the role of HIF-1α in hypoxia-induced Rab22 expression in tubular epithelia, we turned to gene expression-inhibited cells. Therefore, we established HIF-1α and Rab22 knockdown HK2 cells by transfecting HIF-1α and Rab22 siRNA. Compared with negative control (NC), scrambled sequence-transfected cells and HIF-1α siRNA-transfected cells had both lower HIF-1α and Rab22 expressions under hypoxic conditions. However, Rab22 siRNA-transfected cells had only decreased Rab22 expressions. These results indicated

that hypoxia enhanced HIF-1α-dependent Rab22 expression (Fig. 3g, h).

We further tested the HIF-1α- or Rab22-inhibited HK2 cells to investigate the role of the HIF-1α/Rab22 pathway in HPC-induced EV production. We quantified the production of EVs by western blot and ELISA analysis. The no gene expression-inhibited cells under the HPC produced more EV protein HSP70 than cells in normoxia. However, HIF-1α- inhibited cells nearly eliminated the increase in EVs production under the HPC, compared to NC cells. Similarly, the HPC-induced EVs production was also largely attenuated in Rab22-inhibited cells (Fig. 3i, j). Consistently, ELISA analysis indicated that HPC induced the expression of EV protein CD9 was also suppressed in HIF-1α, and Rab22 inhibitedHK2 cells (Fig. 3k). These results revealed that HPC-induced EVs were regulated by the HIF-1α/Rab22 pathway.

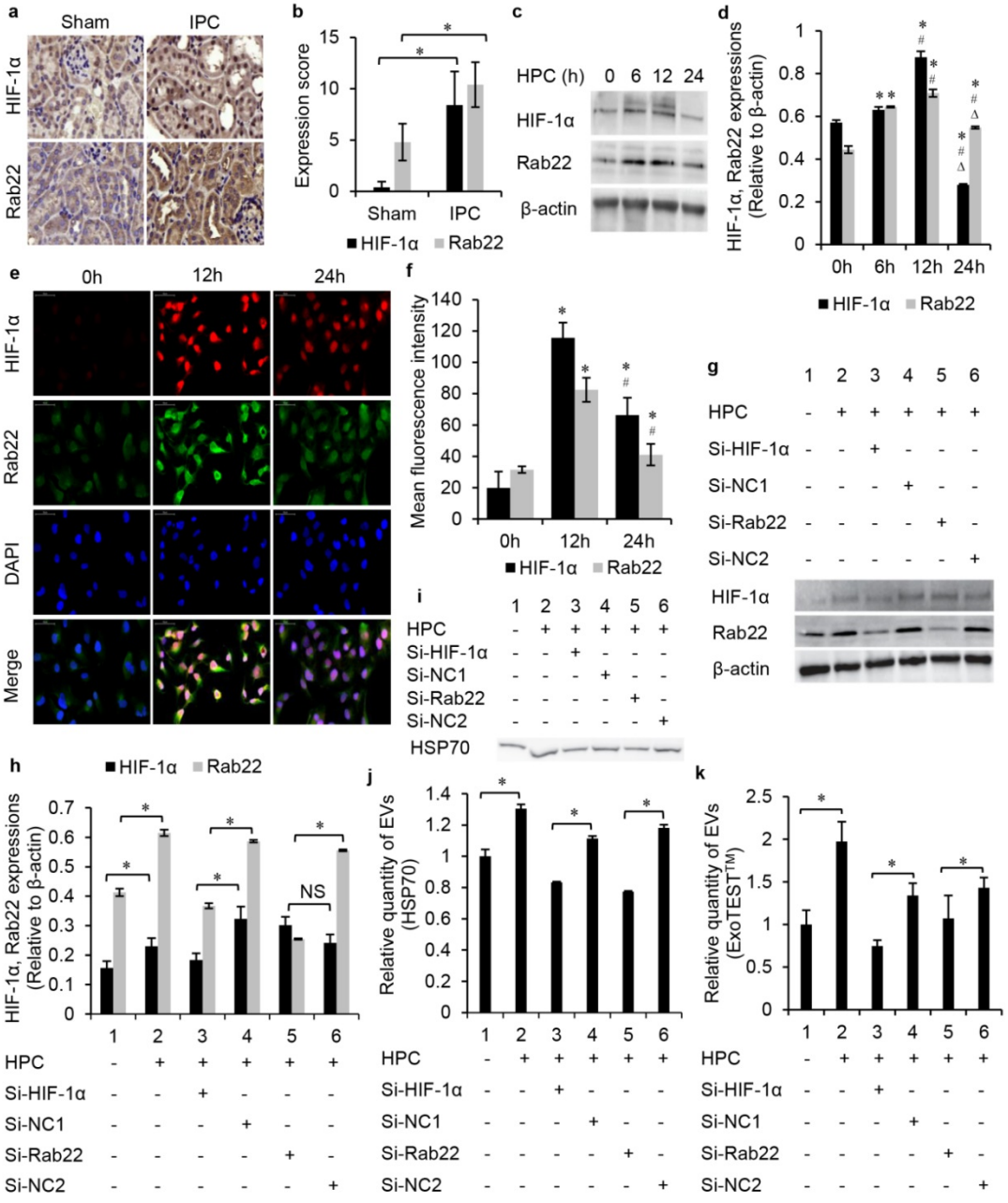

Figure 3. The production of EVs was regulated by the HIF-1α/Rab22 pathway during HPC. (a) Immunohistochemistry staining and (b) semi-quantification analysis of HIF-1α and Rab22 in sham and IPC mice kidneys (magnification 400×, n=5, * P<0.05). (c) Western blot and (d) semi-quantification of HIF-1α and Rab22 expression in cells under HPC (*, #, Δ, P<0.05 compared with 0 h, 6 h, 12 h, respectively). (e) Cellular immunofluorescent assay and (f) semi-quantification of the expression of HIF-1α and Rab22 (*, #, P<0.05 compare with 0 h, 12 h, respectively). (g) Western blot analysis and (h) semi-quantification of the expression of HIF-1α and Rab22 in HIF-1α siRNA-transfected cells, Rab22 siRNA-transfected cells and their negative control (NC) cells under HPC (* P<0.05, NS, no signification). (i) Western blot analysis and (j) semi-quantification of the expression of EVs protein HSP70 in HIF-1α, Rab22 inhibited and NC HK2 cells under HPC (* P<0.05). (k) Relative quantity of EVs in HIF-1α and Rab22 inhibited HK2 cells under HPC by ExoTESTTM analysis (* P<0.05).

HPC EVs were more effective to attenuate mice renal I/R injury than normoxic EVs

To investigate the role of EVs in I/R injury protection, 4 groups of mice models were studied: sham surgery (sham), bilateral renal ischaemia reperfusion injected with PBS (IR+PBS), or with EVs from HK2 cells cultured under normoxic conditions (IR+NOR EV), or with EVs from post hypoxic HK2 cells (IR+HPC EV). To mimic the process that EVs derived from the RTECs during RIPC that we injection the hypoxic EVs before I/R injury, and PKH26 labelled-EVs or PBS vehicle were given intravenously 24 h pre-ischaemia (Fig. 4a). No mortality was observed during the operation.

By PAS staining, we observed that all renal tubules were damaged in the I/R injury group compared with sham surgery animals. After treatment with EVs, the morphological changes of the kidney were alleviated and only the group treated with HPC EVs reached a statistically significant, difference compare with the PBS-treated group (Fig. 4b, c). Renal function was evaluated using serum creatinine (SCr). Results showed Scr levels in sham-operated mice remained within normal limits. In contrast, there was a rapid and similar increase in SCr in all I/R injury groups after 24 hours. Similarly, SCr was lower in the EV-treated group than in the PBS-treated group, and HPC EVs treated group had a significant difference than the PBS-treated group (Fig. 4d). This means that HPC EVs but not the EVs, could significantly improve renal function of ischaemic injured kidneys.

HPC modulated the expression of a subset of miRNAs in EVs

To discover candidate EV-packaged miRNAs (EV-miRNAs) associated with renal protection induced by HPC, we utilized miRNA sequencing for expression profiling of miRNAs in HPC and normoxic cell derived EVs (Table S1). A total of 16 differentially expressed EV-miRNAs (fold change ≥2, P value<0.05) were initially screened, and they were all upregulated in HPC versus the normoxic group. Detailed information of the 16 differentially expressed EV-miRNAs is summarised in Fig. 5.

Prediction and pathway enrichment analysis of target genes of differentially expressed miRNAs

In order to further reveal the role of upregulated EV-miRNAs during HPC, online miRNA prediction databases miRDB, TargetScan and miRWalk were used to identify their putative target genes. The results showed that 438 common putative target genes can regulated by 13 of the dysregulated EV-miRNAs identified in our screen (Fig. 6a), while 3 miRNAs, including miR-127-3p, miR-136-3p and miR-411-5p, had no common predicted genes. Among the dysregulated EV-miRNAs, miR-124-3p had the highest number of target genes with the number of 119, while the others had no more than 60, with the numbers between 6-58 (Fig. 6b).

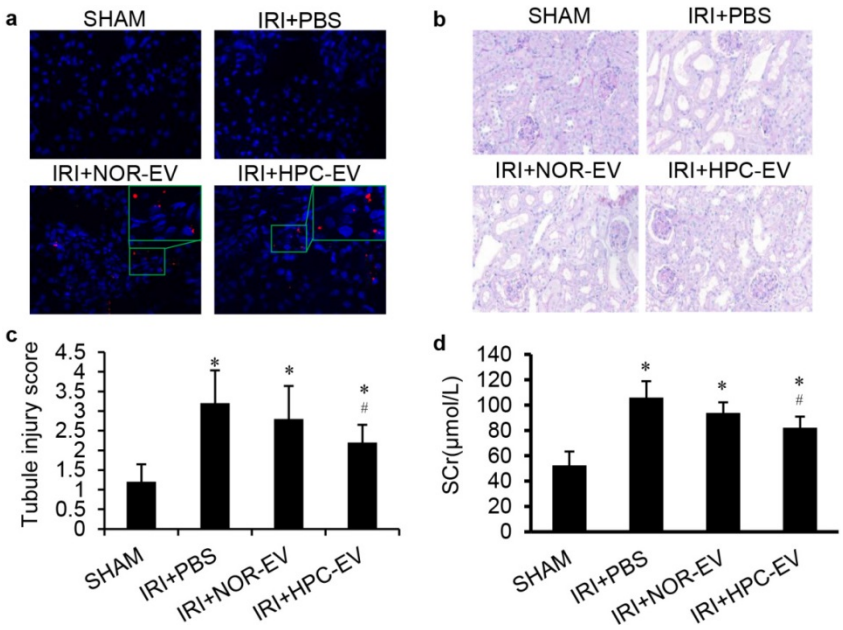

Figure 4. HPC EVs were more effective to attenuate mice renal I/R injury than normoxic EVs. (a) EV tracing in treated IRI kidney, green boxes indicate the location of representative EVs (Red), magnification 400×. (b) Representative renal sections from different groups (PAS staining, magnification 400×). (c) Renal injury scoring and quantitative analysis for different groups. (d) Serum creatinine levels in different groups. (Groups: sham surgery (SHAM), renal ischaemia reperfusion injected with PBS (IR+PBS), with EVs from HK2 cells cultured under normoxic conditions (IR+NOR EV) or with EVs from HPC HK2 cells (IR+HPC EV); *, #, P<0.05 compared with SHAM, IRI+PBS, respectively).

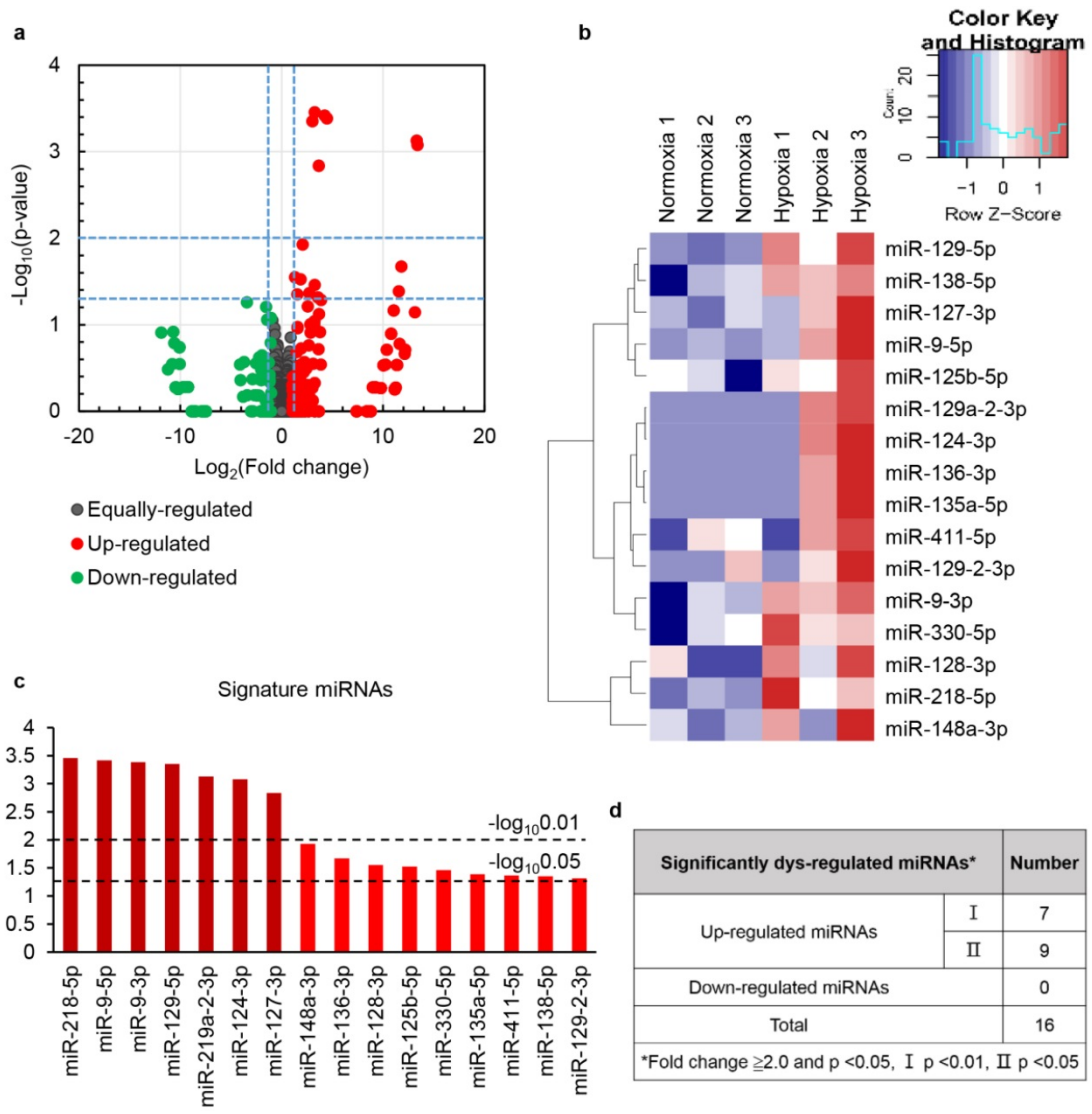

d

Significantly dys-regulated miRNAs*		Number
Up-regulated miRNAs	Ⅰ	7
	Ⅱ	9
Down-regulated miRNAs		0
Total		16

*Fold change ≥2.0 and p <0.05, Ⅰ p <0.01, Ⅱ p <0.05

Figure 5. HPC modulated the expression of a subset of miRNAs in EVs. Differentially expressed miRNAs were analysed by hierarchical clustering of log2 value. Fold change enal ischaemia reperfusion injected with PBS (IR+PBS), with EVs from HK2 cells culturedt (a) for differential gene expression, red and green colours indicate up- or downregulated miRNAs, respectively. The clustered heat map (b), profile (c) and number (d) of the differentially expressed miRNAs are shown.

Furthermore, to determine the potential function of these dysregulated EV-miRNAs, we performed enrichment analysis for the 438 common putative target genes utilizing GO terms. Results associated with these genes were related to the cell proliferation, cellular respiration, transcription, response to dietary excess, stem cell population maintenance, signal transduction, blood vessel development and protein deubiquitination (Fig. 6c), demonstrating that these EV-miRNAs are probably related to I/R injury protection. The target genes of these EV-miRNAs are also primarily located in cytoplasmic stress granule, clathrin-coated vesicle, early endosome, dendritic spine, etc. (Fig. 6d), with transcriptional activator/repressor activity, DNA binding, phosphatidylinositol binding, ATP binding, etc. as the dominating dysfunctional molecular function annotations (Fig. 6e).

We studied the KEGG pathways of selected target genes so as to further uncover the biological function of the EV-miRNAs (Figure. 6f). The most enriched dysfunctional pathways included the insulin signalling pathway, Wnt signalling pathway, FoxO signalling pathway and mTOR signalling pathway, etc. The KEGG pathway analysis reveals the function of the signature EV-miRNAs partly, and signal-related function was highlighted among all the subsystems, which was consistent with GO terms of these selected genes.

Integration of a regulatory network for miRNA-target genes

We assembled and visualised the associations between the miRNAs and target genes by constructing a regulatory network for miRNA-target genes utilizing the Cytoscape. The degree of the

network was defined as the number of edges of a node. The nodes with a higher degree centrality are considered biologically more important genes within the networks. In our study, the higher-degree interactive network contained 9 miRNAs, 15 genes and 31 miRNA-target gene connections (Fig. 7). These genes were target by more than one dys-regulated miRNAs might play more important roles in I/R injury protection.

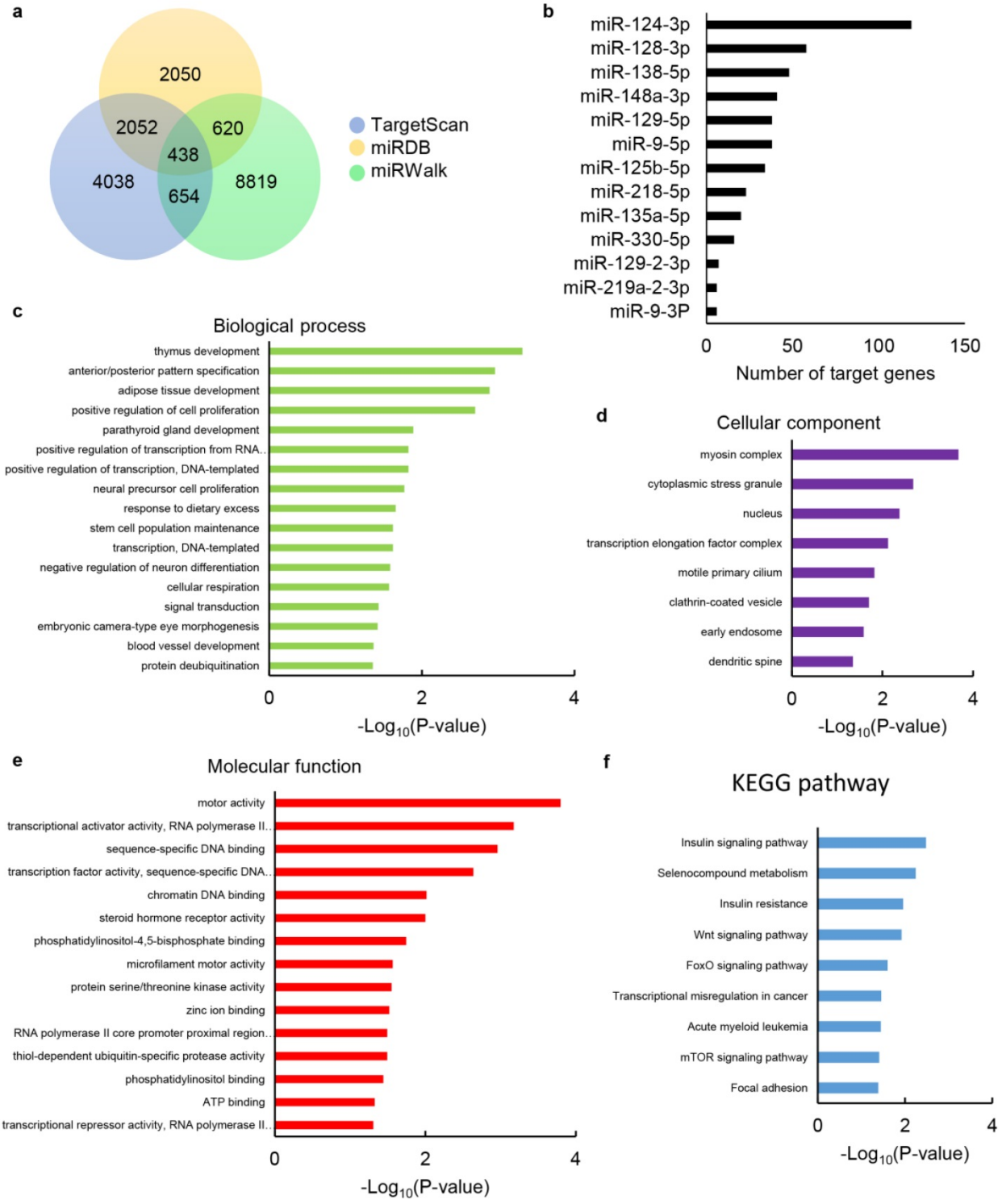

Figure 6. Target gene prediction of differentially expressed miRNAs and bioinformatics analysis of target genes. (a) Venn diagram showing the overlap of candidate target genes. (b) Bar charts showing the number of target genes for dysregulated miRNAs. The chart fragments represent the number of target genes associated with each term. (c) Biological process, (d) cellular components and (e) molecular function assessed by GO analysis. (f) KEGG pathway enrichment analyses for target genes. The terms are listed on the Y-axis, while the P-values are listed on the X-axis.

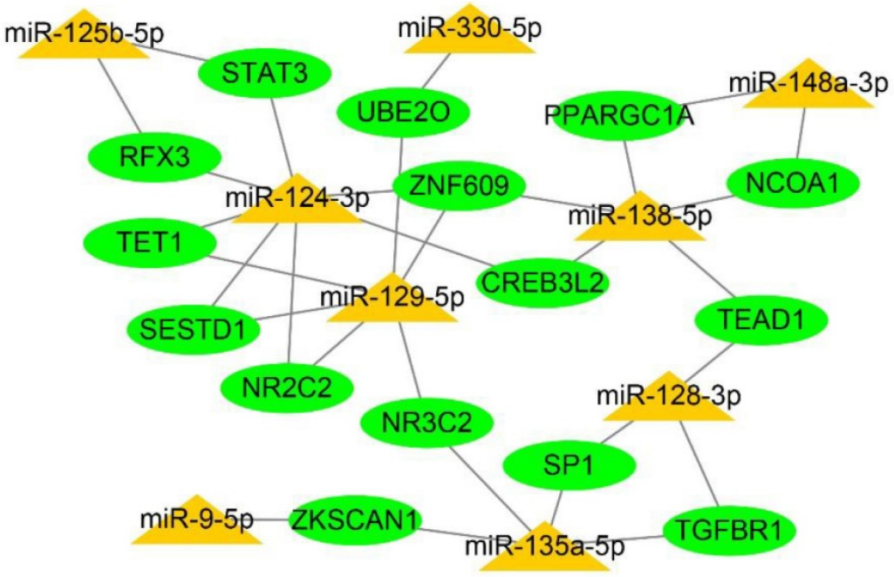

Figure 7. Construction of a regulatory network for integrated miRNA-target genes. The predicted interaction network of miRNAs and target genes was constructed by Cytoscape software. Yellow triangles refer to dysregulated miRNAs, while green elliptic points indicate the target genes.

Discussion

Our previously work was the first to establish a new animal model of RIPC, which was right kidney IPC protecting against I/R injury of left kidney [11]. At approximately the same time, Tuorkey et al. [30] reported a similar kidney RIPC model, demonstrating that kidney RIPC showed better efficacy against I/R injury as a novel and applicable model. We revealed that transient ischaemia/RIPC of right kidney could affect RTECs, making the latter releasing functional EVs to alleviate I/R injury of remote left kidney through the circulatory system in an EV-dependent manner. In the current study, we used human RTECs to simulate RIPC in vitro, indicating that the EV production is enhanced by HPC, This has been further proven to be partly regulated by the HIF-1α/Rab22 pathway. In addition, the HPC cell derived-EVs reveal a protective function of renal I/R injury in mice. Then, miRNAs, one category of the main cargos of EVs are identified to find potentially protective EV-packed miRNAs and their underlying mechanisms.

Multiple pathophysiological responses are believed to contribute to the I/R injury, such as increase of intracellular calcium, pH changes, depletion of adenosine triphosphate, generation of reactive oxygen species (ROS), changes of mitochondrial pore permeability, activation of macrophages and release of pro-inflammatory cytokines, which ultimately from the basis of tissue damage and cellular death [31-33]. Current recognition of cellular ‘‘cross-talk’’ and molecular events have introduced new logical strategies to sequentially combat the events occurring in relation to I/R injury, which includes preconditioning strategies. Actually, either direct or remote IPC, which is a short period of oxygen deprivation and reperfusion, protects various tissues against subsequent sustained ischaemic insults to reduce the extent of injury. Studies have demonstrated that IPC/RIPC can protect organs suffering from I/R injury via promoting cell proliferation and inhibiting cell apoptosis [34-36]. Furthermore, this procedure itself is not considered to cause noteworthy injury to the organs. It has been proven that IPC/RIPC regulates HIF-1α levels and apoptosis to attenuate organ injury [14, 37-39]. Therefore, in the present study, we investigated the optimal conditions to simulate IPC in vitro and focused on cell proliferative and apoptotic events, as well as the regulation of the HIF-1α. We drew the conclusion that optimum conditions to simulate IPC in vitro with HK2 cells were no more than 12 h under the 1% oxygen culture circumstance. Because we observed that hypoxic exposure of HK2 cells within 12 h had no significant effect on proliferation and apoptosis, while the HIF-1α levels in cells increased dramatically and peaked at approximately 12 h.

EVs have recently been proved to play an important role in RIPC-induced protection of the myocardium ischaemic injury [7,40,41]. However, the report on the role of EVs in the RIPC-induced renal ischaemic protective process is still rare. According to our pervious data, we believe that the protective EVs were induced by hypoxia during the process of RIPC. Our present data [11] indicate that EV production in RTECs is increased remarkably during hypoxia, which is consistent with previous studies in

malignant cells [15,16]. Consistently, Borges et al. [42] showed the increase of production of exosome during hypoxia of mouse and human RTECs. Besides, Zhang et al. [43] also evaluated the enhanced production of exosome during hypoxia of rat RTECs by complementary techniques, suggesting the induction of exosomes under hypoxia conditions. Noteworthily, our hypoxia condition was observed to more favourable to the increase of production of the MVs than the exosomes when evaluated by nanoparticle tracking assay. This tendency was not noticed before.

Our work has further demonstrated a crucial role of HIF-1α/Rab22 pathway in EVs production during HPC in HK2 cells. It has been proved that hypoxia-mediated exosome production is HIF-1α-dependent both in malignant cells and benign epithelial cells [15,16,43]. However, the specific downstream target genes whereby HIF-1α regulates EVs under hypoxia is unclear. Wang et al. [16] demonstrated hypoxia-induced increased MVs formation in an HIF/Rab22-dependent manner in breast cancer cells, and Rab22 was proven to be a direct HIF target gene. Inspired by this study, we investigated HIF-1α-dependent Rab22 expression both in vivo and in vitro. Moreover, hypoxia-induced EV production was decreased both in HIF-1α-inhibited and Rab22-inhibited HK2 cells. Together, these results support the role of the HIF-1α/Rab22 pathway in mediating EV biogenesis and secretion in HPC RTECs.

Our previous study has shown that EVs derived from HPC HK2 cells had obvious therapeutic effects for rat renal I/R injury [11]. However, we didn't compare the efficacy with non-HPC EVs. The results cannot be adequately demonstrated that the therapeutic effect was due to HPC implementation. Our current results show that, to mimic RIPC, pre-injection of HPC EVs can significantly attenuate subsequent mice renal I/R injury and improve renal function of I/R injured kidneys rather than normoxic EVs. The results have amply confirmed the unique kidney I/R injury protective function of HPC EVs. Actually, hypoxic cell derived-EVs were always demonstrated to promote tumour growth, invasion and metastasis and were also reported to be pro-fibrotic during kidney fibrosis rather than physiological protection [16,42,44-46]. Consistent with our results, Dominguez et al. [47] showed that EVs from adult rat RTECs successfully treat rats with established severe I/R injury intravenously 24 and 48 h after I/R. Furthermore, EVs from HPC cells were more effective. Taken their and our results together, the HPC EVs derived from RTECs can alleviate both subsequent and established renal I/R injury. Zhang et al. [43] suggested that exosomes from hypoxic RTECs could prevent RTEC apoptosis after ATP depletion. Their study indicated a time window for RTECs to produce cellular protective exosomes under hypoxic exposure. Interestingly, the exosomes extracted during 16 and 24 h of hypoxic exposure were protective, however those extracted from over 24 h of hypoxic exposure were no more protective. This time window in their work further prove the rationality of our choice of optimal conditions of simulate IPC in HK2 cells in turn.

Here, we successfully injected human EVs into immunocompetent mice. Previous studies haven shown that not only allogeneic but also xenogenic EVs could induce some therapeutic effects in immunocompetent small and large animal models, and no significantly acute immune rejection was elicited [48-52]. Possible reasons is that the EVs are acellular therefore likely to be less immunogenic than cells. On the other hand, EVs have been suggested to be able to modulate immunity [53, 54]. Particularly in our study, another possible reason is that normal renal tubular epithelial cells express very low or negative major histocompatibility complex (MHC) Ⅱ and costimulatory molecules (e.g. CD80 and CD86) which impair the activation of immune cells [55, 56]. However, the phenomenon and its specific mechanisms still requires further investigation.

How do the EVs from HPC cells protect renal I/R injury? Our present study does not conclude a clear answer to the question. Nonetheless, HPC may change the cargos of EVs that are considered to be the primary mediators affecting recipient cells [22,46,47]. Our interests focus on miRNAs, because our results show the particular enrichment of small RNAs (about 25 nt) in EVs, and the role of miRNAs in I/R injury has been gradually revealed in recent years. Our study found a total of 16 differentially expressed EV-miRNAs, and all of them were up-regulated in HPC EVs versus normoxic EVs. At present, many of these miRNAs have been reported to play various roles in hypoxic/ischaemic insult (Table S2). Some of the miRNAs have attracted more attentions, some are not. The mechanisms by which these miRNAs act are varied. Sometimes, the effect of the same miRNA might be reported to the contrary conclusion. This suggests that we need to pay more attention to the role of miRNAs in IPC, RIPC or I/R injury. To deepen the understanding of biological functions of these EV-miRNAs, we utilized three online miRNA-target-predicting database (miRBD, TargetScan and miRWalk) to predicte the target genes. Target genes located in the intersection of three databases were chosen for further analyses so that to reduce false positives. Results showed these up-regulated EV-miRNAs were associated with 438

target genes. To further understand the role of these up-regulated miRNAs, pathway enrichment analysis was performed on all 438 genes. Our results indicated that these target genes were involved multiple processes, such as cell proliferation, cellular respiration and transcription. Moreover, multiple pathways, such as the insulin signalling pathway, Wnt signalling pathway, FoxO signaling pathway and mTOR signalling pathway, etc. are involved. These miRNAs are suspected of influencing the corresponding processes and pathways in RIPC/IPC by binding their targets, thereby affecting the consequences of I/R injury. Our miRNA-target gene regulatory network shows that a single miRNA can target multiple genes, and different miRNAs can regulate the same gene. These genes are considered biologically more important genes in the network and are supposed to play more vital roles in I/R injury protection. Signal transducer and activator of transcription 3 (STAT3), was demonstrated to be required and dependent on the RIPC to ameliorate pulmonary I/R injury [57]. Similarly, Wang et al. reported that RIPC attenuated diabetic heart I/R injury by mitigating high glucose-induced protein kinase C (PKC)-ε overexpression and, subsequently, activating STAT3 [58]. Paradoxically, inhibition of STAT3 phosphorylation was reported to promote neurological function recovery following ischaemic stroke by RIPC treatment or epigenetically regulated with miR-126a [59,60]. Inhibiting specificity protein 1 (SP1) by miR-374 could exert protective effects by activating the phosphatidylinositol-4,5-bisphosphate 3-kinase/protein kinase B (PI3K/AKT) pathway in rat models of myocardial I/R after sevoflurane preconditioning [61]. However, another study revealed that EVs from human-induced pluripotent stem cell-derived mesenchymal stromal cells (hiPSC-MSCs) protect against kidney I/R injury via transmitting SP1, and transcriptional activating of sphingosine kinase 1 and inhibiting necroptosis [62]. In addition to these studies, peroxisome Proliferator-Activated Receptor Gamma Coactivator 1 Alpha (PPARGC1A), a well characterised positive regulator of mitochondrial function and oxidative metabolism has been shown to regulate oxidative stress, which is directly associated with IPC and I/R injury [63,64]. Inhibiting the expression of nuclear receptor coactivator 1 (NRCOA1) has been shown to reduce inflammation and apoptosis and thus protect the rat and cell models of cerebral I/R injury [65]. Huang et al. [66] reported that I/R injury influenced DNA hydroxymethylation and tet methylcytosine dioxygenase 1 (TET1) gene expression in mouse kidneys, which may contribute to the regulation of gene transcription during renal I/R injury. Recently, there have been several reports about the role of related genes in preconditioning or I/R injury. However, some conclusions about the role of genes are actually contradictory, and there are still many genes involved in preconditioning or I/R injury that remain to be studied further. In short, the function of the differentially expressed EV-miRNAs and their target genes in RIPC-induced renal I/R injury protection remain largely unknown. Further insight to these regulatory mechanisms will facilitate to the management of renal I/R injury.

Limitations in our study should be noted. Firstly, we tried to uncover the mechanism of RIPC to alleviate renal I/R injury by producing protective EVs through simulation of IPC in vitro. However, the actual biochemical reactions in vivo are quite complex, and the conditions in vitro are still very different. Secondly, due to the limitations of hardware and funding, we used the transient transfected cells rather than stable HIF-1α, Rab22-deficient or over-expressed cell lines, which partly influenced the persuasion of the experimental results. In addition, the reliability of our results would be greatly enhanced if renal-specific HIF-1α and Rab22 knockdown animal models were studied. However, it is still difficult to say the production of IPC EVs depends entirely on HIF-1α and the downstream pathway because many transcription factors as well as cellular signalling pathways are activated during RIPC that may mediate the effect. Moreover, EVs play a biological regulatory role through their nucleic acid, protein and other contents, although our focus was only on miRNAs. Lastly, these differentially expressed miRNAs, regardless of their expression, function and underlying mechanism, need to be further verified in vitro and in vivo in the future.

In summary, in this study, we demonstrated that the HIF-1α/Rab22 pathway regulated the production of RETC-derived EVs during RIPC. The HPC EVs protected renal I/R injury potentially through differentially expressed EV-miRNAs. Further study is needed to verify the effective EV-miRNAs and underlying mechanism.

Supplementary Material

Supplementary figures and tables.
http://www.ijbs.com/v15p1161s1.pdf

Acknowledgements

This work was supported by grants from National Natural Science Foundation of China (NO. 81670632), Health and Family Planning Commission of Jiangsu Province Foundation (Z201609), grants of Jiangsu Provincial Medical Youth Talent, Six Talent Peaks Project in Jiangsu Province, Jiangsu Provincial

Medical Innovation Team (CXTDA2017025), Jiangsu Provincial Medical Talent (ZDRCA2016080), Jiangsu Provincial Medical Youth Talent (QNRC2016821, QRNC2016820), Fundamental Research Funds for the Central Universities and Scientific Research Innovation Program for College and University Graduates of Jiangsu Province (KYCX17_0180). Lei Zhang thanks the China Scholarship Council (CSC) for scholarship support (No. 201706090205). We thank WebShop (webshop.elsevier.com) for its linguistic assistance during the preparation of this manuscript.

Competing Interests

The authors have declared that no competing interest exists.

References

1. Siew ED, Davenport A. The growth of acute kidney injury: a rising tide or just closer attention to detail? Kidney Int. 2015; 87: 46-61.
2. Fan H, Yang HC, You L, Wang YY, He WJ, Hao CM. The histone deacetylase, SIRT1, contributes to the resistance of young mice to ischemia/reperfusion-induced acute kidney injury. Kidney Int. 2013; 83: 404-13.
3. Murry CE JR, Reimer KA. Preconditioning with ischemia A delay of lethal cell injury in ischemic myocardium. Circulation. 1986; 74: 1124-36.
4. Takaoka A, Nakae I, Mitsunami K, Yabe T, Morikawa S, Inubushi T, et al. Renal ischemia/reperfusion remotely improves myocardial energy metabolism during myocardial ischemia via adenosine receptors in rabbits: effects of "remote preconditioning". J Am Coll Cardiol. 1999; 33: 556-64.
5. Moretti C, Cerrato E, Cavallero E, Lin S, Rossi ML, Picchi A, et al. The EUROpean and Chinese cardiac and renal Remote Ischemic Preconditioning Study (EURO-CRIPS CardioGroup I): A randomized controlled trial. Int J Cardiol. 2018; 257: 1-6.
6. Wang Y, Meng R, Song H, Liu G, Hua Y, Cui D, et al. Remote Ischemic Conditioning May Improve Outcomes of Patients With Cerebral Small-Vessel Disease. Stroke. 2017; 48: 3064-72.
7. Giricz Z, Varga ZV, Baranyai T, Sipos P, Paloczi K, Kittel A, et al. Cardioprotection by remote ischemic preconditioning of the rat heart is mediated by extracellular vesicles. J Mol Cell Cardiol. 2014; 68: 75-8.
8. Ma F, Liu H, Shen Y, Zhang Y, Pan S. Platelet-derived microvesicles are involved in cardio-protective effects of remote preconditioning. Int J Clin Exp Pathol. 2015; 8: 10832-9.
9. Colombo M, Raposo G, Thery C. Biogenesis, secretion, and intercellular interactions of exosomes and other extracellular vesicles. Annu Rev Cell Dev Biol. 2014; 30: 255-89.
10. Lawson C, Kovacs D, Finding E, Ulfelder E, Luis-Fuentes V. Extracellular Vesicles: Evolutionarily Conserved Mediators of Intercellular Communication. Yale J Biol Med. 2017; 90: 481-91.
11. Zhang G, Yang Y, Huang Y, Zhang L, Ling Z, Zhu Y, et al. Hypoxia-induced extracellular vesicles mediate protection of remote ischemic preconditioning for renal ischemia-reperfusion injury. Biomed Pharmacother. 2017; 90: 473-8.
12. Semenza GL. Hypoxia-inducible factor 1: regulator of mitochondrial metabolism and mediator of ischemic preconditioning. Biochim Biophys Acta. 2011; 1813: 1263-8.
13. Yang J, Liu C, Du X, Liu M, Ji X, Du H, et al. Hypoxia Inducible Factor 1alpha Plays a Key Role in Remote Ischemic Preconditioning Against Stroke by Modulating Inflammatory Responses in Rats. J Am Heart Assoc. 2018; 7.
14. Albrecht M, Zitta K, Bein B, Wennemuth G, Broch O, Renner J, et al. Remote ischemic preconditioning regulates HIF-1alpha levels, apoptosis and inflammation in heart tissue of cardiosurgical patients: a pilot experimental study. Basic Res Cardiol. 2013; 108: 314.
15. King HW, Michael MZ, Gleadle JM. Hypoxic enhancement of exosome release by breast cancer cells. BMC Cancer. 2012; 12: 421.
16. Wang T, Gilkes DM, Takano N, Xiang L, Luo W, Bishop CJ, et al. Hypoxia-inducible factors and RAB22A mediate formation of microvesicles that stimulate breast cancer invasion and metastasis. Proc Natl Acad Sci U S A. 2014; 111: E3234-42.
17. Bhuin T, Roy JK. Rab proteins: the key regulators of intracellular vesicle transport. Exp Cell Res. 2014; 328: 1-19.
18. Hutagalung AH, Novick PJ. Role of Rab GTPases in membrane traffic and cell physiology. Physiol Rev. 2011; 91: 119-49.
19. Croce C, Mayorga LS, Cebrian I. Differential requirement of Rab22a for the recruitment of ER-derived proteins to phagosomes and endosomes in dendritic cells. Small GTPases. 2017: 1-9.
20. Meng Y, Eirin A, Zhu XY, O'Brien DR, Lerman A, van Wijnen AJ, et al. The metabolic syndrome modifies the mRNA expression profile of extracellular vesicles derived from porcine mesenchymal stem cells. Diabetol Metab Syndr. 2018; 10: 58.
21. Eirin A, Zhu XY, Puranik AS, Woollard JR, Tang H, Dasari S, et al. Comparative proteomic analysis of extracellular vesicles isolated from porcine adipose tissue-derived mesenchymal stem/stromal cells. Sci Rep. 2016; 6: 36120.
22. Shao C, Yang F, Miao S, Liu W, Wang C, Shu Y, et al. Role of hypoxia-induced exosomes in tumor biology. Mol Cancer. 2018; 17: 120.
23. Li M, Zeringer E, Barta T, Schageman J, Cheng A, Vlassov AV. Analysis of the RNA content of the exosomes derived from blood serum and urine and its potential as biomarkers. Philos Trans R Soc Lond B Biol Sci. 2014; 369.
24. Keasey MP, Scott HL, Bantounas I, Uney JB, Kelly S. MiR-132 Is Upregulated by Ischemic Preconditioning of Cultured Hippocampal Neurons and Protects them from Subsequent OGD Toxicity. J Mol Neurosci. 2016; 59: 404-10.
25. Xu X, Kriegel AJ, Liu Y, Usa K, Mladinov D, Liu H, et al. Delayed ischemic preconditioning contributes to renal protection by upregulation of miR-21. Kidney Int. 2012; 82: 1167-75.
26. Wei Q, Liu Y, Liu P, Hao J, Liang M, Mi QS, et al. MicroRNA-489 Induction by Hypoxia-Inducible Factor-1 Protects against Ischemic Kidney Injury. J Am Soc Nephrol. 2016; 27: 2784-96.
27. Lorenzen JM, Kaucsar T, Schauerte C, Schmitt R, Rong S, Hubner A, et al. MicroRNA-24 antagonism prevents renal ischemia reperfusion injury. J Am Soc Nephrol. 2014; 25: 2717-29.
28. Liu KX, Chen Q, Chen GP, Huang JC, Huang JF, He XR, et al. Inhibition of microRNA-218 reduces HIF-1alpha by targeting on Robo1 in mice aortic endothelial cells under intermittent hypoxia. Oncotarget. 2017; 8: 104359-66.
29. Chen GH, Xu CS, Zhang J, Li Q, Cui HH, Li XD, et al. Inhibition of miR-128-3p by Tongxinluo Protects Human Cardiomyocytes from Ischemia/reperfusion Injury via Upregulation of p70s6k1/p-p70s6k1. Front Pharmacol. 2017; 8: 775.
30. Tuorkey MJ. Kidney remote ischemic preconditioning as a novel strategy to explore the accurate protective mechanisms underlying remote ischemic preconditioning. Interv Med Appl Sci. 2017; 9: 20-6.
31. Kalogeris T, Baines CP, Krenz M, Korthuis RJ. Ischemia/Reperfusion. Compr Physiol. 2016; 7: 113-70.
32. Kalogeris T, Baines CP, Krenz M, Korthuis RJ. Cell biology of ischemia/reperfusion injury. Int Rev Cell Mol Biol. 2012; 298: 229-317.
33. Yellon DM, Hausenloy DJ. Myocardial reperfusion injury. N Engl J Med. 2007; 357: 1121-35.
34. Zhang C, Rosenbaum DM, Shaikh AR, Li Q, Rosenbaum PS, Pelham DJ, et al. Ischemic preconditioning attenuates apoptotic cell death in the rat retina. Invest Ophthalmol Vis Sci. 2002; 43: 3059-66.
35. Damous LL, Silva SM, Carbonel AA, Simoes Mde J, Baracat EC, Montero EF. Progressive Evaluation of Apoptosis, Proliferation, and Angiogenesis in Fresh Rat Ovarian Autografts Under Remote Ischemic Preconditioning. Reprod Sci. 2016; 23: 803-11.
36. Zhao R, Feng J, He G. Hypoxia increases Nrf2-induced HO-1 expression via the PI3K/Akt pathway. Front Biosci (Landmark Ed). 2016; 21: 385-96.
37. Weber NC, Riedemann I, Smit KF, Zitta K, van de Vondervoort D, Zuurbier CJ, et al. Plasma from human volunteers subjected to remote ischemic preconditioning protects human endothelial cells from hypoxia-induced cell damage. Basic Res Cardiol. 2015; 110: 17.
38. Xia M, Ding Q, Zhang Z, Feng Q. Remote Limb Ischemic Preconditioning Protects Rats Against Cerebral Ischemia via HIF-1alpha/AMPK/HSP70 Pathway. Cell Mol Neurobiol. 2017; 37: 1105-14.
39. Eckle T, Kohler D, Lehmann R, El Kasmi K, Eltzschig HK. Hypoxia-inducible factor-1 is central to cardioprotection: a new paradigm for ischemic preconditioning. Circulation. 2008; 118: 166-75.
40. Minghua W, Zhijian G, Chahua H, Qiang L, Minxuan X, Luqiao W, et al. Plasma exosomes induced by remote ischaemic preconditioning attenuate myocardial ischaemia/reperfusion injury by transferring miR-24. Cell Death Dis. 2018; 9: 320.
41. Yamaguchi T, Izumi Y, Nakamura Y, Yamazaki T, Shiota M, Sano S, et al. Repeated remote ischemic conditioning attenuates left ventricular remodeling via exosome-mediated intercellular communication on chronic heart failure after myocardial infarction. Int J Cardiol. 2015; 178: 239-46.
42. Borges FT, Melo SA, Ozdemir BC, Kato N, Revuelta I, Miller CA, et al. TGF-beta1-containing exosomes from injured epithelial cells activate fibroblasts to initiate tissue regenerative responses and fibrosis. J Am Soc Nephrol. 2013; 24: 385-92.
43. Zhang W, Zhou X, Yao Q, Liu Y, Zhang H, Dong Z. HIF-1-mediated production of exosomes during hypoxia is protective in renal tubular cells. Am J Physiol Renal Physiol. 2017; 313: F906-F13.
44. Xue M, Chen W, Xiang A, Wang R, Chen H, Pan J, et al. Hypoxic exosomes facilitate bladder tumor growth and development through transferring long non-coding RNA-UCA1. Mol Cancer. 2017; 16: 143.
45. Li L, Li C, Wang S, Wang Z, Jiang J, Wang W, et al. Exosomes Derived from Hypoxic Oral Squamous Cell Carcinoma Cells Deliver miR-21 to Normoxic Cells to Elicit a Prometastatic Phenotype. Cancer Res. 2016; 76: 1770-80.
46. Chen X, Zhou J, Li X, Wang X, Lin Y, Wang X. Exosomes derived from hypoxic epithelial ovarian cancer cells deliver microRNAs to macrophages and elicit a tumor-promoted phenotype. Cancer Lett. 2018; 435: 80-91.
47. Dominguez JH, Liu Y, Gao H, Dominguez JM, 2nd, Xie D, Kelly KJ. Renal Tubular Cell-Derived Extracellular Vesicles Accelerate the Recovery of

Established Renal Ischemia Reperfusion Injury. J Am Soc Nephrol. 2017; 28: 3533-44.
48. Zou X, Kwon SH, Jiang K, Ferguson CM, Puranik AS, Zhu X, et al. Renal scattered tubular-like cells confer protective effects in the stenotic murine kidney mediated by release of extracellular vesicles. Sci Rep. 2018; 8: 1263.
49. Zhao B, Zhang Y, Han S, Zhang W, Zhou Q, Guan H, et al. Exosomes derived from human amniotic epithelial cells accelerate wound healing and inhibit scar formation. J Mol Histol. 2017; 48: 121-32.
50. Beltrami C, Besnier M, Shantikumar S, Shearn AI, Rajakaruna C, Laftah A, et al. Human Pericardial Fluid Contains Exosomes Enriched with Cardiovascular-Expressed MicroRNAs and Promotes Therapeutic Angiogenesis. Mol Ther. 2017; 25: 679-93.
51. Gallet R, Dawkins J, Valle J, Simsolo E, de Couto G, Middleton R, et al. Exosomes secreted by cardiosphere-derived cells reduce scarring, attenuate adverse remodelling, and improve function in acute and chronic porcine myocardial infarction. Eur Heart J. 2017; 38: 201-11.
52. Zhou Y, Xu H, Xu W, Wang B, Wu H, Tao Y, et al. Exosomes released by human umbilical cord mesenchymal stem cells protect against cisplatin-induced renal oxidative stress and apoptosis in vivo and in vitro. Stem Cell Res Ther. 2013; 4: 34.
53. de Castro LL, Xisto DG, Kitoko JZ, Cruz FF, Olsen PC, Redondo PAG, et al. Human adipose tissue mesenchymal stromal cells and their extracellular vesicles act differentially on lung mechanics and inflammation in experimental allergic asthma. Stem Cell Res Ther. 2017; 8: 151.
54. Reis M, Ogonek J, Qesari M, Borges NM, Nicholson L, Preussner L, et al. Recent Developments in Cellular Immunotherapy for HSCT-Associated Complications. Front Immunol. 2016; 7: 500.
55. Muczynski KA, Ekle DM, Coder DM, Anderson SK. Normal human kidney HLA-DR-expressing renal microvascular endothelial cells: characterization, isolation, and regulation of MHC class II expression. J Am Soc Nephrol. 2003; 14: 1336-48.
56. Niemann-Masanek U, Mueller A, Yard BA, Waldherr R, van der Woude FJ. B7-1 (CD80) and B7-2 (CD 86) expression in human tubular epithelial cells in vivo and in vitro. Nephron. 2002; 92: 542-56.
57. Luo N, Liu J, Chen Y, Li H, Hu Z, Abbott GW. Remote ischemic preconditioning STAT3-dependently ameliorates pulmonary ischemia/reperfusion injury. PLoS One. 2018; 13: e0196186.
58. Wang C, Li H, Wang S, Mao X, Yan D, Wong SS, et al. Repeated Non-Invasive Limb Ischemic Preconditioning Confers Cardioprotection Through PKC-/STAT3 Signaling in Diabetic Rats. Cell Physiol Biochem. 2018; 45: 2107-21.
59. Cheng X, Zhao H, Yan F, Tao Z, Wang R, Han Z, et al. Limb remote ischemic post-conditioning mitigates brain recovery in a mouse model of ischemic stroke by regulating reactive astrocytic plasticity. Brain Res. 2018; 1686: 94-100.
60. Tian YS, Zhong D, Liu QQ, Zhao XL, Sun HX, Jin J, et al. Upregulation of miR-216a exerts neuroprotective effects against ischemic injury through negatively regulating JAK2/STAT3-involved apoptosis and inflammatory pathways. J Neurosurg. 2018: 1-12.
61. Zhang SB, Liu TJ, Pu GH, Li BY, Gao XZ, Han XL. MicroRNA-374 Exerts Protective Effects by Inhibiting SP1 Through Activating the PI3K/Akt Pathway in Rat Models of Myocardial Ischemia-Reperfusion After Sevoflurane Preconditioning. Cell Physiol Biochem. 2018; 46: 1455-70.
62. Yuan X, Li D, Chen X, Han C, Xu L, Huang T, et al. Extracellular vesicles from human-induced pluripotent stem cell-derived mesenchymal stromal cells (hiPSC-MSCs) protect against renal ischemia/reperfusion injury via delivering specificity protein (SP1) and transcriptional activating of sphingosine kinase 1 and inhibiting necroptosis. Cell Death Dis. 2017; 8: 3200.
63. Hu L, Zhou L, Wu X, Liu C, Fan Y, Li Q. Hypoxic preconditioning protects cardiomyocytes against hypoxia/reoxygenation injury through AMPK/eNOS/PGC-1alpha signaling pathway. Int J Clin Exp Pathol. 2014; 7: 7378-88.
64. Sanchez-Ramos C, Prieto I, Tierrez A, Laso J, Valdecantos MP, Bartrons R, et al. PGC-1alpha Downregulation in Steatotic Liver Enhances Ischemia-Reperfusion Injury and Impairs Ischemic Preconditioning. Antioxid Redox Signal. 2017; 27: 1332-46.
65. Yu H, Wu M, Zhao P, Huang Y, Wang W, Yin W. Neuroprotective effects of viral overexpression of microRNA-22 in rat and cell models of cerebral ischemia-reperfusion injury. J Cell Biochem. 2015; 116: 233-41.
66. Huang N, Tan L, Xue Z, Cang J, Wang H. Reduction of DNA hydroxymethylation in the mouse kidney insulted by ischemia reperfusion. Biochem Biophys Res Commun. 2012; 422: 697-702.